*Supporting Information*

# Catalyst-free Growth of Two-Dimensional $BC_xN$ Materials on Dielectrics by Temperature-Dependent Plasma-Enhanced Chemical Vapor Deposition

Kongyang Yi, [†,‡,‖] Zhepeng Jin, [†,‡] Saiyu Bu,[§] Dingguan Wang,[¶] Donghua Liu,[†,‡] Yamin Huang,[‖] Yemin Dong,[‖] Qinghong Yuan,[§] Yunqi Liu,[‡] Andrew Thye Shen Wee[¶] and Dacheng Wei[†,‡,*]

[†]State Key Laboratory of Molecular Engineering of Polymers, Department of Macromolecular Science, Fudan University, Shanghai 200433, China

[‡]Institute of Molecular Materials and Devices, Fudan University, 200433 Shanghai, China.

[§] State Key Laboratory of Precision Spectroscopy, School of Physics and Electronic Science, East China Normal University, 3663 N. Zhongshan Road, Shanghai 200062, China.

[¶]Department of Physics, National University of Singapore, 2 Science Drive 3, Singapore 117542, Singapore.

[‖] State Key Laboratory of Functional Materials for Informatics, Shanghai Institute of Microsystem and Information Technology, Chinese Academy of Sciences, Shanghai 200092, China.

**Corresponding author. E-mail: weidc@fudan.edu.cn;*

**First-principles calculations**

First-principles calculations, based on density functional theory, were performed using the Vienna Ab initio Simulation Package (VASP).[1,2] The projector-augmented-wave (PAW)[3,4] method was used to mimic the ionic cores. The electronic exchange

and correlation were included through the generalized gradient approximation (GGA) in the Perdew–Burke–Ernzerhof (PBE)[5] form. The plane-wave cutoff energy for the wave function was set to 450 eV. All structures were optimized by a conjugate gradient method until the energy was converged to $1.0\times10^{-5}$ eV/atom and the minimum energy path was optimized using a force-based conjugate-gradient method until the force was converged to 0.01 eV/Å. The thickness of the vacuum slab layer was set to 15 Å to avoid interaction between adjacent unit cells. Brillouin zone integration was approximated by a sum over special selected *k*-points using the Monkhorst-Pack method[6] and k-point mesh used for the model was set as 10×6×1. Since PBE seriously underestimated the band gap, the screened hybrid functional of Heyd, Scuseria, and Ernzerhof (HSE06)[7] was used to calculate the electronic properties.

**References**


1. Kresse, G.; Furthmüller, J. Efficient Iterative Schemes for ab initio Total-Energy Calculations Using a Plane-Wave Basis Set. *Phys. Rev. B* **1996**, *54*, 11169–11186.
2. Kresse, G.; Furthmiiller, J. Efficiency of ab-initio Total Energy Calculations for Metals and Semiconductors Using a Plane-Wave Basis Set. *Comput. Mater. Sci.* **1996**, *6*, 15–50.
3. Han, F. Projector-Augmented Plane-Wave Method. *Probl. Solid State Phys. with Solut.* **2012**, *50*, 391–396.
4. Kresse, G.; Joubert, D. From Ultrasoft Pseudopotentials to the Projector

Augmented-Wave Method. *Phys. Rev. B* **1999**, *59*, 11–19.

5. Perdew, J. P.; Burke, K.; Ernzerhof, M. Generalized Gradient Approximation Made Simple. *Phys. Rev. Lett.* **1996***, 77*, 3865–3868.

6. Hendrik J. Monkhorst. Special Points for Brillouin-Zone Integretions. *Phys. Rev. B* **1976**, *13*, 5188–5192.

7. Heyd, J.; Scuseria, G. E.; Ernzerhof, M. Hybrid Functionals Based on a Screened Coulomb Potential. *J. Chem. Phys.* **2003**, *118*, 8207–8215.

**Table S1.** Influence of parameters on growth other than growth temperature.

| $BH_3 \cdot NH_3$ (°C) | $CH_4/H_2/Ar$ (sccm) | Growth time (min) | Plasma power (W) | B/C/N (at%) | Morphology |
|---|---|---|---|---|---|
| 105 | 3/0/50 | 30 | 30 | 24.8/55.1/20.1 | thick film |
| 115 | 3/10/50 | 30 | 30 | 34.3/40.3/25.4 | thick film |
| 105 | 3/10/50 | 30 | 30 | 25/48/27 | 2D film |
| 105 | 3/10/0 | 30 | 30 | 28.1/47.7/24.2 | thick film |
| 105 | 3/10/50 | 30 | 50 | 30.2/43.4/26.4 | thick film |

*All samples were grown at 600 °C.

Influence of parameters including precursor ratio, flow rate and plasma power on the growth were demonstrated (Table S1). When $H_2$ was absent, C content was slightly higher than the case when $H_2$ was incorporated, and thick film was obtained, indicating the role of etching by $H_2$ during growth. When the evaporating temperature of $BH_3 \cdot NH_3$ was elevated to 115 °C, more B and N sources were provided compared with C source. Higher BN content was observed in the thick film, indicating a stronger deposition of BN in the growth. When the carrier gas Ar was removed, the plasma density was increased due to the dramatically lowered air pressure, favoring the deposition and leading to the formation of the thick film. When plasma power was increased to 50 W, the growth rate was increased, resulting in the thick film.

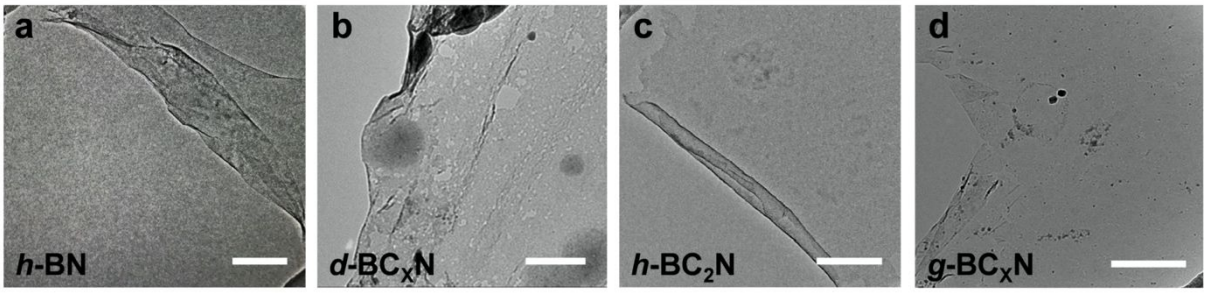


**Figure S1.** TEM images of e) *h*-BN, f) *d*-$BC_xN$ (0<x<2), g) *h*-$BC_2N$, h) *g*-$BC_xN$ (x>2) films. Scale bars, 200 nm in (e), (f), (g) and (h).

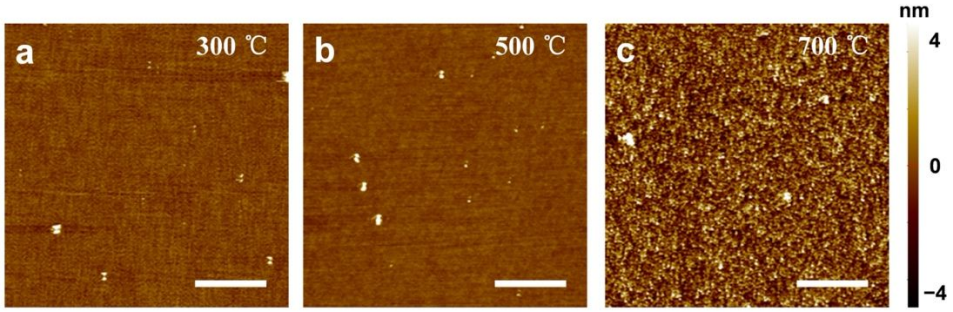


**Figure S2.** AFM images of samples grown at a) 300 °C, b) 500 °C, c) 700 °C. Scale bars, 500 nm.

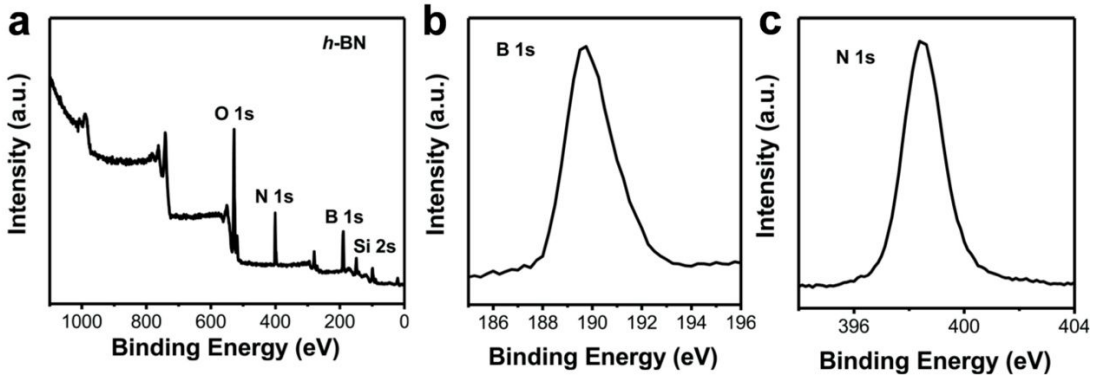


**Figure S3.** a) Full-range XPS spectrum of 2D *h*-BN. XPS b) B 1s and c) N1s spectra of 2D *h*-BN.

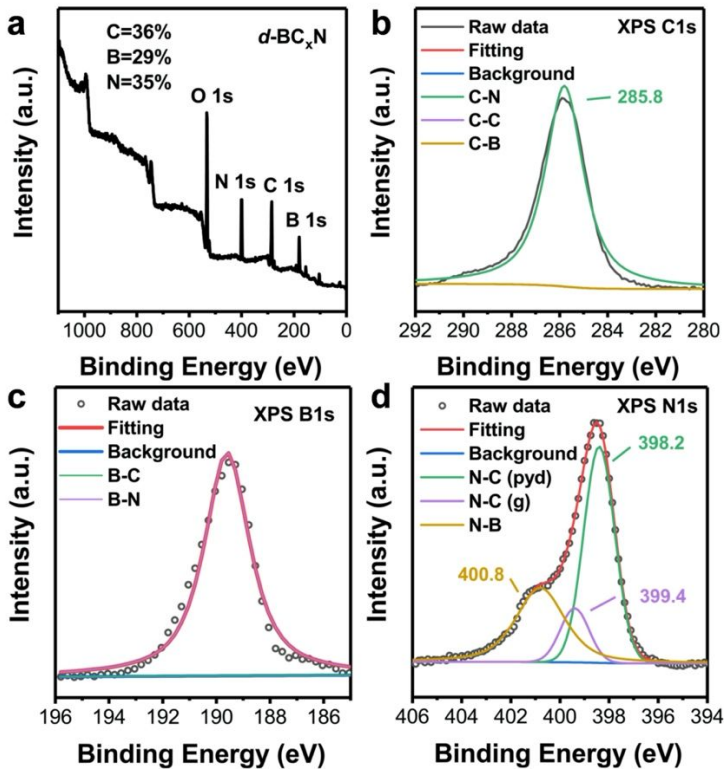


**Figure S4.** a) Full-range XPS spectrum of *d*-$BC_xN$. XPS b) C 1s, c) B 1s, d) N 1s spectra of *d*-$BC_xN$.

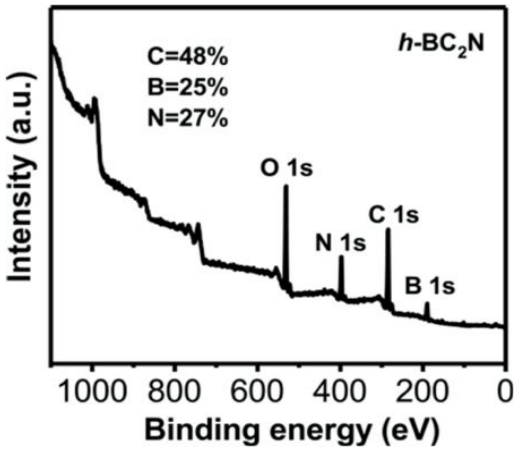


**Figure S5.** Full-range XPS spectrum acquired from 2D *h*-$BC_2N$ film grown on $SiO_2$/Si.

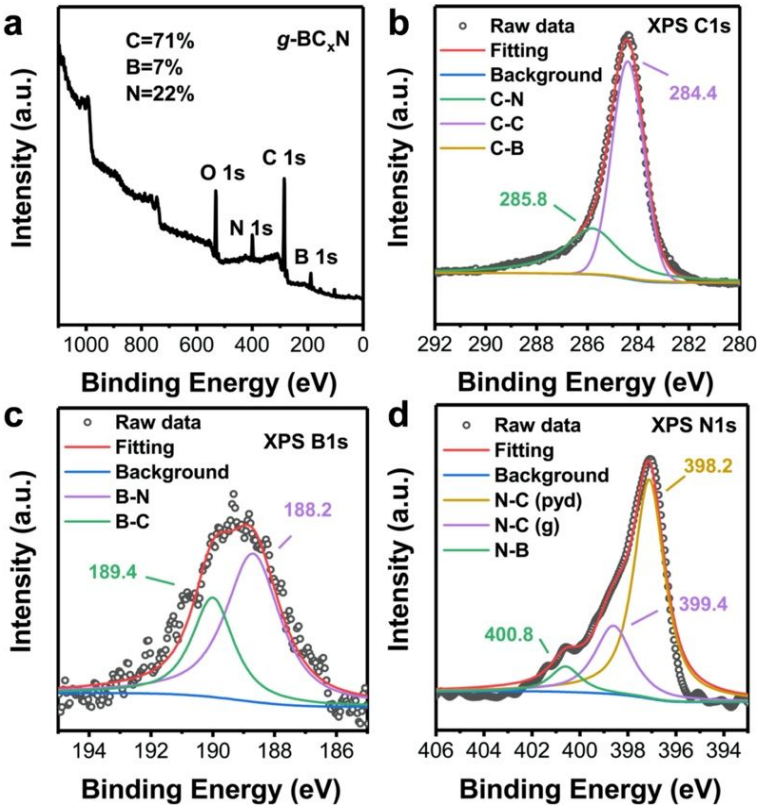


**Figure S6.** a) Full-range XPS spectrum of *g*-$BC_xN$. XPS b) C 1s, c) B 1s, d) N 1s spectra of *g*-$BC_xN$.

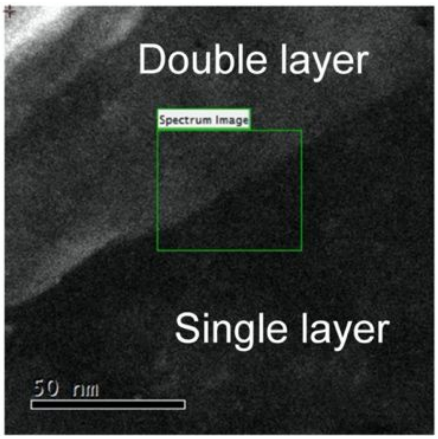


**Figure S7.** Bright field STEM image of 2D *h*-$BC_2N$ film. The selected area is the scanned area of EELS mapping.

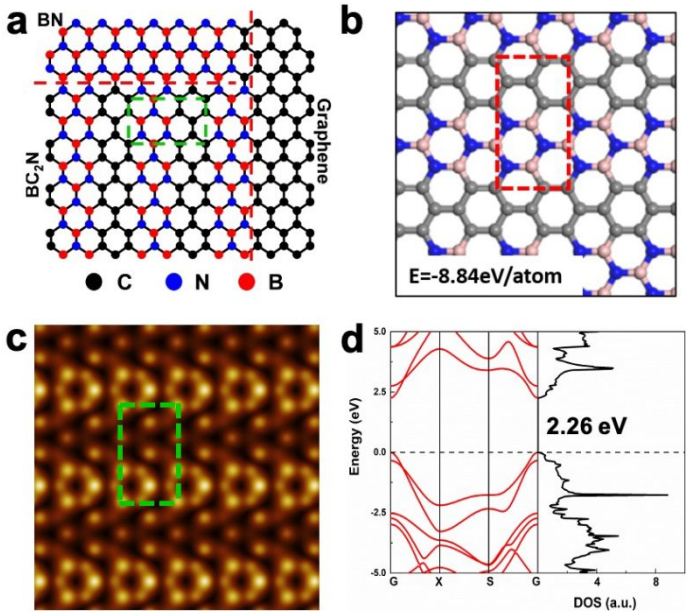


**Figure S8.** (a) Atomic model of *h*-$BC_2N$ film showing ideal atomic arrangement (green dash lines). (b) A possible structure of 2D $BC_2N$ (red dash lines representing a repeating unit). (c) STM simulation of an ideal $BC_2N$. (d) Band structures and density of states of (c) calculated by HSE06.